General Disclaimer

One or more of the Following Statements may affect this Document

- This document has been reproduced from the best copy furnished by the organizational source. It is being released in the interest of making available as much information as possible.

- This document may contain data, which exceeds the sheet parameters. It was furnished in this condition by the organizational source and is the best copy available.

- This document may contain tone-on-tone or color graphs, charts and/or pictures, which have been reproduced in black and white.

- This document is paginated as submitted by the original source.

- Portions of this document are not fully legible due to the historical nature of some of the material. However, it is the best reproduction available from the original submission.

DOE/NASA/1028-78/15
NASA TM-73883

EXPERIMENTAL DATA AND THEORETICAL ANALYSIS OF AN OPERATING 100 kW WIND TURBINE

Bradford S. Linscott and John Glasgow
National Aeronautics and Space Administration
Lewis Research Center
Cleveland, Ohio 44135

and

William D. Anderson and Robert E. Donham
Lockheed California Company
Burbank, California

Work performed for
DEPARTMENT OF ENERGY
Division of Solar Energy
Federal Wind Energy Program
Under Interagency Agreement E(49-26)-1028

TECHNICAL PAPER presented at the
Twelfth Intersociety Energy Conversion Engineering Conference
sponsored by the American Nuclear Society
Washington, D.C., August 28 - September 2, 1977

1. Report No. NASA TM-73883	2. Government Accession No.	3. Recipient's Catalog No.
4. Title and Subtitle EXPERIMENTAL DATA AND THEORETICAL ANALYSIS OF AN OPERATING 100 kW WIND TURBINE		5. Report Date January 1978 6. Performing Organization Code
7. Author(s) Bradford S. Linscott and John Glasgow, Lewis Research Center, Cleveland, Ohio; and William D. Anderson and Robert E. Donham, Lockheed California Co., Burbank, Calif.		8. Performing Organization Report No. E-9496 10. Work Unit No.
9. Performing Organization Name and Address National Aeronautics and Space Administration Lewis Research Center Cleveland, Ohio 44135		11. Contract or Grant No. 13. Type of Report and Period Covered
12. Sponsoring Agency Name and Address Department of Energy Division of Solar Energy Washington, D.C. 20545		14. Sponsoring Agency ~~Code~~ Report No. DOE/NASA/1028-78/15

15. Supplementary Notes

Prepared under Interagency Agreement E(49-26)-1028. This paper presented at the Twelfth Intersociety Energy Conversion Engineering Conference, Washington, D.C., August 28-September 2, 1977.

16. Abstract

Various studies have indicated that Wind Energy has the potential to make significant contributions to the Nation's energy needs. The level of contribution depends on the initial and operating costs of the machines which can convert wind energy to electricity or other forms of energy useful to the public. Part of the cooperative effort between NASA and the Energy Research and Development Agency (ERDA) has been the design and the erection of an experimental wind turbine by the NASA-Lewis Research Center. This 100 kW turbine, designated the Mod-0, is located at the NASA Plum Brook site near Sandusky, Ohio. Experimental test data have been correlated with analyses of turbine loads and complete system behavior of the ERDA-NASA 100 kW Mod-0 wind turbine generator over a broad range of steady state conditions, as well as during transient conditions. The deficit in the ambient wind field due to the upwind tower turbine support structure was found to be very significant in exciting higher harmonic loads associated with the flapping response of the blade in bending.

17. Key Words (Suggested by Author(s))	18. Distribution Statement Unclassified - unlimited STAR Category 44 DOE Category UC-60

19. Security Classif. (of this report)	20. Security Classif. (of this page)	21. No. of Pages	22. Price*
Unclassified	Unclassified		

* For sale by the National Technical Information Service, Springfield, Virginia 22161

EXPERIMENTAL DATA AND THEORETICAL ANALYSIS OF AN OPERATING 100 kW WIND TURBINE*

Bradford S. Linscott
Deputy Manager Mod 1, 1500 kW Wind Tubrine

John Glasgow
Manager Mod-0, 100 kW Wind Turbine

NASA Lewis Research Center
Cleveland, Ohio

William D. Anderson
Manager - Mod-0 Dynamics Analysis

Robert E. Donham
Project Engineer - Mod-0 Metal Blades

Lockheed California Company
Burbank, California

Abstract

Various studies have indicated that Wind Energy has the potential to make significant contributions to the Nation's energy needs. The level of contribution depends on the initial and operating costs of the machines which can convert wind energy to electricity or other forms of energy useful to the public.

Part of the cooperative effort between NASA and the Energy Research and Development Agency (ERDA) has been the design and the erection of an experimental wind turbine by the NASA-Lewis Research Center. This 100 kW turbine, designated the Mod-0, is located at the NASA Plum Brook site near Sandusky, Ohio.

Experimental test data have been correlated with analyses of turbine loads and complete system behavior of the ERDA-NASA 100 kW Mod-0 wind turbine generator over a broad range of steady state conditions, as well as during transient conditions.

The deficit in the ambient wind field due to the upwind tower turbine support structure was found to be very significant in exciting higher harmonic loads associated with the flapping response of the blade in bending.

NOTATION

E = modulus of elasticity, lb/in.^{2}
G = shear modulus of elasticity, lb/in.^{2}
g = damping coefficient
I = area moment of inertia, in.^{4}
J = polar moment of inertia, in.^{4}
K = torsional stiffness, in.-lb/deg
r = radial blade dimension, in.
R = blade radius at tip, in.
V_w = wind velocity, mi/hr
θ = blade pitch angle, deg
ω_n = natural frequency, rad/sec
Ω = rotational velocity, rad/sec

INTRODUCTION

Recent shortages in the supply of clean energy, coupled with increasing costs of fuel, have forced the nation to reassess all forms of energy, including wind power, to determine their practicality. In January 1975, the responsibility for the nation's wind-energy program was assigned to the newly formed energy agency, Energy Research and Development Administration (ERDA). Under the overall program, the NASA-Lewis Research Center (LeRC) provides project management for a portion of that program.

The NASA-LeRC wind energy program includes the (1) design and operation of a 100-kW experimental wind turbine generator (WTG), (2) program management of industry-designed and user operated WTG's in the 50 to 3,000 kilowatt range, and (3) development of supporting research and technology for WTG energy systems.

To meet this objective, LeRC selected a 100-kW WTG as being large enough to assess technology and solve engineering problems of large (1 - 3 megawatts) WTG's and yet to maintain costs within the available project budget. The test program provides engineering data needed to determine whether the technology for wind energy can be used to create machines that will help meet the nation's energy needs at costs that are competitive with other systems.

Test results obtained during the period from October 1975 through April 1976, while the air flow was blocked by the tower stairs, have been correlated with analyses. The first effort to provide test/analysis correlation was carried out by the Lockheed California Company under NASA sponsorship, Contract NAS3-20036; the results of this contracted study are extensively reported in this paper.

A marked improvement in porosity of the tower has been achieved by removal of the tower stairs and rails. The test results of this current Mod-0 configuration shows that substantial reductions in blade flap bending loadings are obtained. A second improvement in the Mod-0 system has been the incorporation of a dual yaw-drive/brake-system which eliminates free play in the yaw axis. This benefits the yaw system structurally and also reduces blade inplane blade loadings.

*Presented at the Twelfth Intersociety Energy Conversion Engineering Conference, Washington, D.C., August 28-September , 1977.

The Mod-0 test/analysis program is providing the engineering data necessary to support the development of wind turbine technology while directly solving the real engineering problems experienced with the Mod-0 machine. Analyses must account for the tower flexibility/rotor system in a fully-coupled description to accurately predict loadings.

SUMMARY

Configuration Effects on Rotor Blade Loads. Three sequential configuration evolutions have resulted in the current Mod-0 wind turbine. For each of the three configurations, the wind turbine was operationally tested in a similar wind environment. The purpose for the tests was primarily to compare rotor blade loads as a function of structural configuration, while attempting to maintain an identical wind environment.

Configuration I - The wind turbine tower is configured with stairs and rails as shown in Figure 1. A single yaw drive is installed between the tower and the nacelle as described in reference 1.

Configuration II - The wind turbine tower stairs and rails are removed, as shown in Figure 2. The single yaw drive between the tower and the nacelle is retained.

Figure 1. Mod-0 Wind Turbine - Original Configuration with Stairs and Rails.

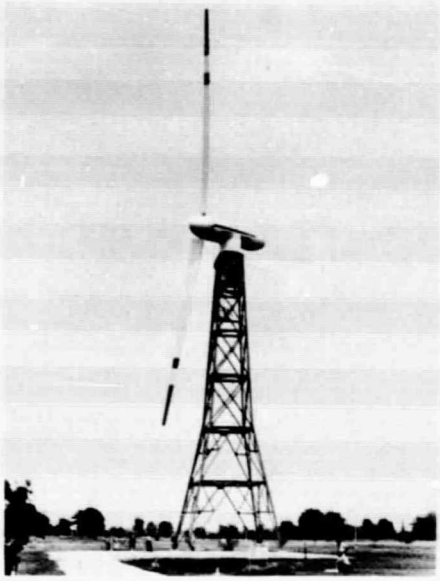

Figure 2. Mod-0 Wind Turbine - Current Configuration without Stairs or Rails

Configuration III - The wind turbine tower stairs and rails are removed. A mechanical lock (yaw keeper) is installed between the nacelle and tower structure. The yaw keeper provides much higher torsional stiffness in yaw rotation than the single yaw drive. This has been mechanically incorporated by design and installation of a dual yaw actuation drive combined with a brake system, see Figures 3 and 4.

Synoptically, the results that these configuration changes achieved on the wind turbine blade root bending moments (measured at 40 inches from the shaft center line) are summarized on Table I.

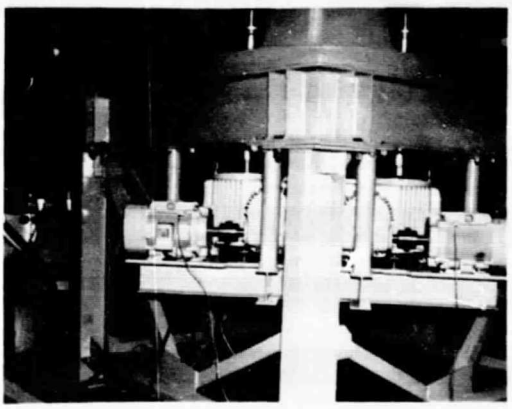

Figure 3. Mod-0 Wind Turbine - Current Configuration Dual Yaw Drive, Motors and Gear Boxes

TABLE I. BLADE BENDING MOMENTS MEASURED DURING OPERATION IN CONFIGURATIONS I, II AND III COMPARED WITH THE DESIGN LOADS

MOD O OPERATIONAL CONFIGURATION	BLADE BENDING MOMENT (FT-LBS) AT STATION 40					
	FLAPWISE			INPLANE		
	PEAK TO PEAK	MEAN	CYCLIC	PEAK TO PEAK	MEAN	CYCLIC
CONFIG I	130,000	−65,000	±65,000	108,000	−18,000	±54,000
CONFIG. II	70,000	−17,850	±35,000	102,850	−10,280	±51,420
CONFIG. III	64,500	−7,750	±32,250	80,000	−18,000	±40,000
DESIGN	58,000	−23,400	±29,000	75,000	−11,200	±37,500

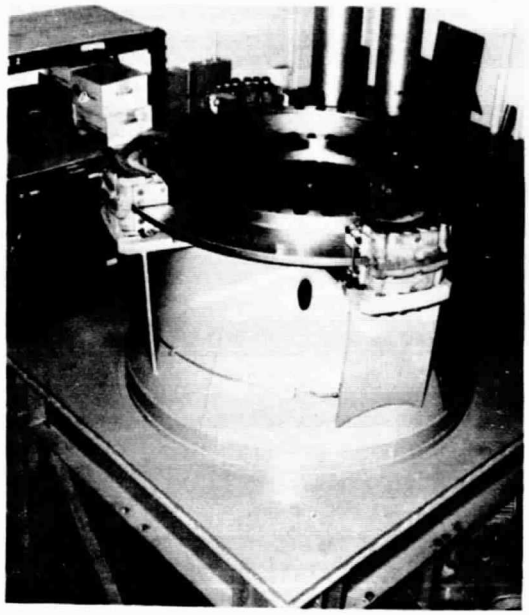

Figure 4. Mod-0 Wind Turbine Current Configuration Yaw Drive Disc Brakes

The supporting tests and correlations which were conducted with analytical methods and which lead to the understanding and solution of these engineering problems is the primary subject of this paper. To facilitate a more detailed examination into the structural dynamics of the Mod-0 wind turbine system Appendix A has been included which provides basic Mod-0 geometry, mass and stiffness distributions, blade frequency spectra, and tower wake test results by NASA LeRC and Lockheed, also see references 2, 3 and 4.

The blade loading measurements taken for configurations I, II and III, presented in Table I, were obtained with power loadings into a resistive load. Synchronous operation with emphasis on the power/drive train dynamics is reported following this discussion.

Rotor Loads for Configuration I. As reported in reference 2, the Mod-0 rotor was operating at 40 rpm, the wind velocity was 26 mph with an inflow angle of 10 degrees and the wind turbine was producing 100 kW of power on the resistive load bank. The Configuration I operating conditions for the blade loads are shown in Table I. These loads are significantly higher than the loads used to design the blades, reference 3, for 50,000 hours of operating life, also shown in Table I.

A visual inspection was conducted, by NASA, on each blade to detect any surface cracks or deformations. No surface irregularities were found.

The character of the loading in flap bending at station 40 clearly indicates that a strong tower shadow effect was present, see Figure 5. The large pulse flap bending upwind, approximately forty-five (45) degrees past vertical (down) in the direction of rotation, is due to wake velocity deficiency behind the tower which results in large (12 degree) thrusting incremental angle of attack.

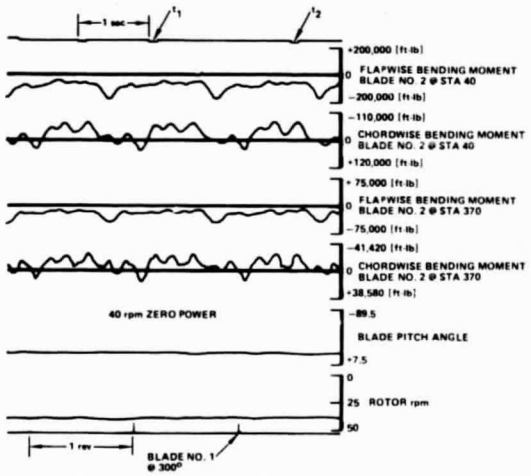

Figure 5. Configuration I of Mod-0, 40 RPM, 100 KW

The Lockheed California Company, designer and fabricator of the Mod-0 metal blades, was funded under Contract NAS 3-20036 by the NASA-Lewis Research Center to evaluate the test data and conduct structural analyses of the wind turbine rotor blade to provide:

Task I - Fatigue Analysis

Task II - Analysis of Wind Velocity Measurement Test Data

Task III - Correlation of Analytical with Actual Loads Data

Task IV - Potential Structural Blade Modification

Lockheed applied two different analytic computer programs to determine loads for correlation with measured data supplied by NASA: Lockheed's WINTUR (WINd TURbine) program, a quasi-steady fully-coupled analysis method (a brief description of the method is included in Reference 2); and an adaptation of Lockheed's REXOR-WT (Revised and EXtended rotOR-Wind Turbine) program.

Loads computed by the WINTUR program were used to calculate loads used in the fatigue analysis, Task I. The test conditions for which correlation was shown are:

- 40 rpm and 100 kW, see Figures 6 and 7
- 40 rpm and zero power
- 30 rpm and zero power
- 20 rpm and zero power
- Emergency feathering

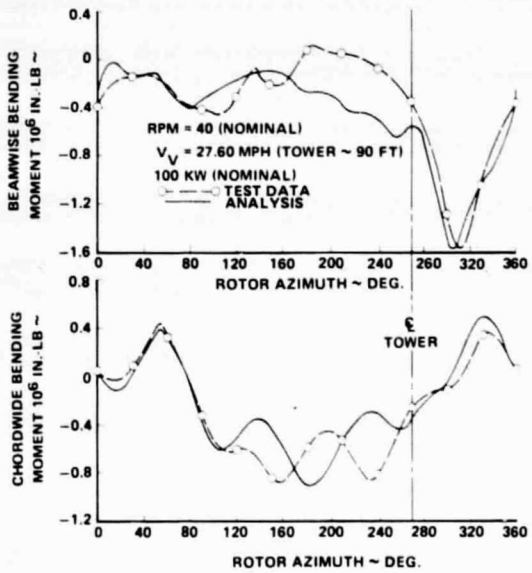

Figure 6. Correlation of Blade Bending Moment Between Test Data and Analysis for NASA MOD-0 100 kW Wind Turbine

THEORETICAL ANALYSIS

The REXOR-WT model provides for a variable-rotor-speed, fully-coupled, non-linear aerostructural-dynamic simulation of the wind turbine system. The equations of motion use the Lagrange energy approach. The simulation includes a complete large-motion non-linear periodic coefficient representation of the blades and the asymmetric description of the tower-pylon-shaft system. The model is capable of simulating nonlinear spring, damper and control system characteristics. The blade loadings, inertial and aerodynamic, are defined in this study as 13

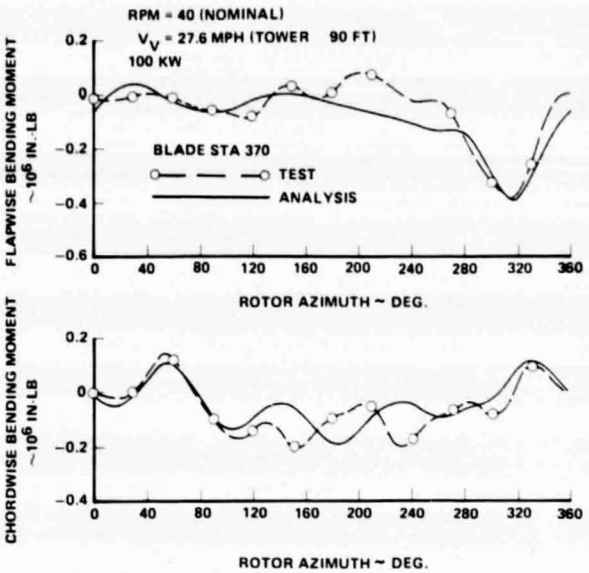

Figure 7. Correlation of Blade Bending Moment Between Test and Analysis for NASA MOD-0 100 kW Wind Turbine

radial panels. Aeroelastic analyses (divergence, flutter and stall) of rotating and stopped rotor blades are presented in Reference 5. For added clarity of the general dynamic analysis of the coupled rotor-tower system, including consideration of order analysis of the nonlinear case, see References 6 and 7.

The wind shear modeled in the program (actually in both the WINTUR and REXOR-WT programs) was defined by the equation

$$V_w(r, \psi, t) = V_{w_{REF}}(t) \left(\frac{H(r,\psi)}{H_{REF}}\right)^{\eta}$$

where H is the distance above the ground, varying with radial position, r, and azimuth indexing, ψ, of each blade. H_{REF} is the reference altitude at which the wind velocity is defined. A value of η = 0.2 was used.

Tower shadow data for this study was supplied by NASA from wind tunnel model tests. A comparison of the wind tunnel data with a simplified approximation used in the model and with test data from Task II which was supplied by Lockheed's Huntsville facility is shown on Figure 8. The comparison is good. The analytic representation in the model is a simple triangular pattern which has a thirty degree azimuthal sector width and 100 percent retardation of the wind at the peak of the triangle, directly behind the tower. The pattern is shown in the following sketch:

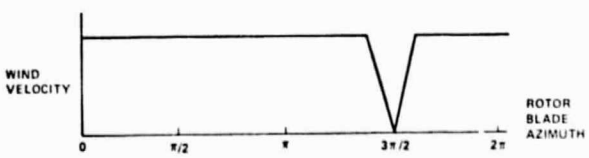

The REXOR-WT solution method is a stepwise time history. The time step of integration is one-fortieth to one-sixtieth of the period of the

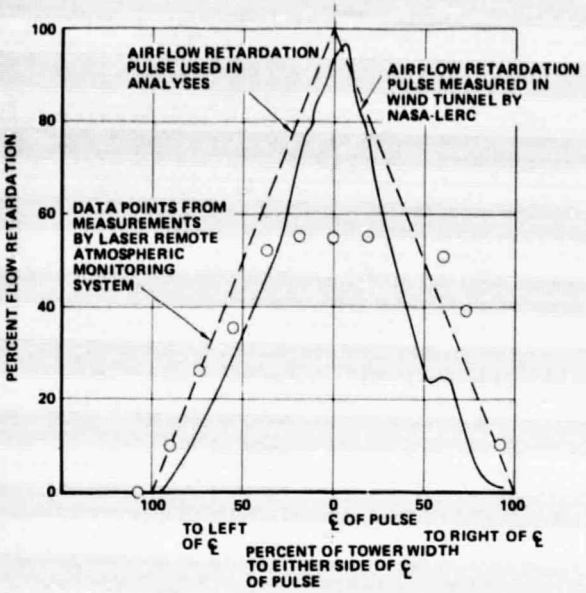

Figure 8. Comparison of Measured Flow Retardation With Pulse Used in Analyses (at approx. 0.8R)

highest system dynamic frequency. A comparison of experiment, WINTUR, and REXOR-WT results is shown on Tatle II.

Introducing tower flexibility generally improved the correlation except for 5P chordwise bending moments. The effect of tower flexibility was to improve correlation of the 3P and 5P flapwise bending moments and (in particular) the 3P chordwise moments. The flexible tower analysis tends to overpredict 2P flap and chord moments. Examination of time histories indicated this was due primarily to the control system feeding 2P collective oscillations into the system.

As expected, freeing the rotor shaft has a significant effect on 4P chord moments. A very significant effect was also seen in the 5P chord moments. The fixed shaft analysis tended to underpredict these moments by a factor of two whereas the flexible tower/shaft analysis apparently caused a tuning of the system to 5P, resulting in overprediction of the 5P chord moments by a factor of two.

This tuning effect means that these loads are critically dependent on assumptions regarding structural damping on the blades, tower and nacelle as well as the accuracy of modelling the structural dynamics of the nacelle/tower. An analysis with the nacelle yaw-degree-of-freedom locked out resulted in a large change of the predicted 5P inplane moments at station 40 from 526,000 in-lb to 40,200 in-lb. This indicates that these loads are very dependent upon both stiffness and damping of the nacelle yaw system.

An over-plot showing the effect of rigidizing the nacelle yaw drive on inplane bending moments is shown in Figure 9.

More correlation data are presented in Tables II through VI. Shown in these tables is a comparison

TABLE II. COMPARISON OF REXOR AND WINTUR ANALYSIS RESULTS AND EXPERIMENTAL DATA - 0 kW, 40 RPM

HARMONIC / LOAD/SOURCE	0P	1P		2P		3P		4P		5P	
	AMP	AMP	ϕ	AMP	ϕ	AMP	ϕ	AMP	ϕ	AMP	ϕ
STA 40 FLAP (IN-LB)											
REXOR (1)	-934,000	294,000	118°	345,000	5°	236,000	114°	63,000	86°	90,000	45°
REXOR (2)	-901,000	376,500	118°	231,700	20°	165,000	5°	51,000	80°	36,500	45°
WINTUR (2)	-988,500	410,000	121°	240,000	30°	228,000	19°	74,000	7°	60,000	60°
EXPERIMENTAL (3)	-954,000	320,000	154°	230,000	34°	290,000	8°	99,000	85°	110,000	52°
STA 40 "INPLANE" (IN-LB)											
REXOR (1)	-245,000	467,000	0°	88,200	1°	225,000	59°	15,000	82°	526,000	46°
REXOR (2)	-238,000	451,000	3°	11,100	56°	49,000	59°	230,000	34°	93,000	47°
WINTUR (2)	-245,000	451,000	3°	7,800	61°	67,000	78°	278,300	55°	122,000	62°
EXPERIMENTAL (3)	-307,000	450,000	350°	48,000	23°	220,000	52°	112,000	25°	247,000	45°
STA 370 FLAP (IN-LB)											
REXOR (1)	-243,000	74,800	115°	102,000	7°	79,400	117°	21,600	89°	38,000	52°
REXOR (2)	-231,000	97,600	118°	66,700	23°	52,300	8°	20,900	83°	15,200	50°
WINTUR (2)	-256,000	108,000	120°	69,500	32°	66,600	21°	22,700	10°	18,700	64°
EXPERIMENTAL (3)	-219,000	71,000	155°	59,600	31°	88,000	3°	32,000	80°	37,000	52°
STA 370 CHORD (IN-LB)											
REXOR (1)	-72,000	87,500	4°	30,500	4°	56,100	58°	2,600	80°	178,000	47°
REXOR (2)	-66,300	83,700	9°	7,000	38°	13,000	57°	70,500	34°	28,300	48°
WINTUR (2)	-59,300	81,200	8°	6,100	40°	18,200	78°	84,000	55°	34,100	62°
EXPERIMENTAL (3)	-104,000	93,000	347°	23,000	20°	61,000	49°	37,000	23°	90,000	44°

NOTES: (1) FLEXIBLE TOWER/SHAFT AND ACTIVE PITCH CONTROL SYSTEM
(2) FIXED SHAFT
(3) APPROXIMATE READING ACCURACY:
STA 40 FLAP ±30,000 IN-LB; INPLANE ±18,000
STA 370 FLAP ±12,000 IN-LB; CHORD ±6,000

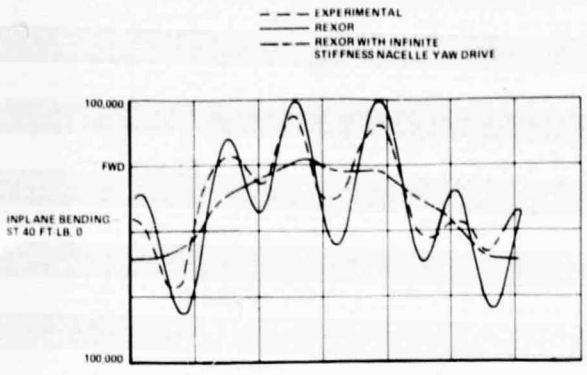

Figure 9. 100 kW - 40 rpm Time History Rexor - Wt

of the harmonics of flap and chordwise bending moments and rotor shaft torque for the 0 kW - 40 rpm, the 100 kW - 40 rpm, the 0 kW - 30 rpm, and the 0 kW - 20 rpm "steady" operating conditions. The comparison shows experimental data and results of the REXOR simulation. Table III is a repeat of the data of Table II, except that shaft torque is added.

In reviewing recorded shaft torque, theoretically, harmonics of 1P, 3P, 5P, etc., should be zero, yet experimental data shows magnitudes of these odd harmonics of the same order as the even harmonics. This raises questions as to the accuracy of the shaft torque experimental data examined in these studies or that the control system is pumping in extraneous frequency excitation.

TABLE III. MOD-0 CORRELATION STUDY - 0 kW, 40 RPM

HARMONIC / LOAD	0P	1P		2P		3P		4P		5P	
	AMP	AMP	ϕ	AMP	ϕ	AMP	ϕ	AMP	ϕ	AMP	ϕ
STA 40 FLAP (IN-LB)											
ANALYSIS	−934,000	294,000	118°	345,000	5°	236,000	114°	63,000	86°	90,000	45°
EXP	−954,000	320,000	154°	230,000	34°	290,000	8°	99,000	85°	110,000	52°
STA 40 CHORD (IN-LB)											
ANALYSIS	−245,000	467,000	0°	88,200	1°	225,000	59°	15,000	82°	526,000	46°
EXP	−307,000	450,000	350°	48,000	23°	220,000	52°	112,000	25°	247,000	45°
STA 370 FLAP (IN-LB)											
ANALYSIS	−243,000	74,800	115°	102,000	7°	79,400	117°	21,600	89°	38,000	52°
EXP	−219,000	71,000	155°	59,600	31°	88,000	3°	32,000	80°	37,000	52°
STA 370 CHORD (IN-LB)											
ANALYSIS	−72,000	87,500	4°	30,500	4°	56,100	58°	2,600	80°	178,000	47°
EXP	−104,000	93,000	347°	23,000	20°	61,000	49°	37,000	23°	90,000	44°
SHAFT TORQUE (IN-LB)											
ANALYSIS	−87	170	4°	19,200	88°	1,050	2°	27 000	40°	540	45°
EXP	−6,200	18,300	315°	24,700	47°	31,800	75°	26,000	26°	24,000	70°

TABLE IV. MOD-0 CORRELATION STUDY - 100 kW, 40 RPM

HARMONIC / LOAD	0P	1P		2P		3P		4P		5P	
	AMP	AMP	ϕ	AMP	ϕ	AMP	ϕ	AMP	ϕ	AMP	ϕ
STA 40 FLAP (IN-LB)											
ANALYSIS	−398,000	341,700	106°	368,000	13°	249,000	−12°	99,600	−20°	106,900	48°
EXP	−373,000	361,000	151°	380,000	36°	192,000	16°	85,400	0°	105,000	58°
STA 40 CHORD (IN-LB)											
ANALYSIS	−214,500	464,600	−5°	51,700	8°	239,000	60°	73,000	70°	454,000	46°
EXP	−271,000	504,000	4°	56,200	28°	171,700	67°	29,200	57°	153,000	54°
STA 370 FLAP (IN-LB)											
ANALYSIS	−77,600	92,200	105°	108,000	16°	84,400	−8°	28,700	70°	52,000	5·
EXP	−63,200	97,400	143°	108,200	32°	52,000	11°	31,100	84°	38,600	61°
STA 370 CHORD (IN-LB)											
ANALYSIS	−48,700	86,900	−2°	19,500	11°	59 500	60°	21,500	69°	157,000	46°
EXP	−59,000	98,000	6°	33,400	28°	46,200	66°	14,400	60°	54,400	54°
SHAFT TORQUE (IN-LB)											
ANALYSIS	−284,000	8,900	195°	33,400	98°	16,900	70°	32,500	−18°	8,350	5°
EXP	−319,000	18,700	349°	27,500	33°	13,700	91°	34,900	9°	7,500	43°

TABLE V. MOD-0 CORRELATION STUDY - 0 kW, 30 RPM

HARMONIC / LOAD	0P	1P		2P		3P		4P		5P	
	AMP	AMP	Φ	AMP	Φ	AMP	Φ	AMP	Φ	AMP	Φ
STA 40 FLAP (IN-LB)											
ANALYSIS	-571,000	188,000	123°	116,000	4°	110,700	10°	85,900	77°	68,000	50°
EXP	567,000	316,000	126°	106,000	-6°	143,000	-13°	140,000	62°	67,000	50°
STA 40 CHORD (IN-LB)											
ANALYSIS	-122,000	447,000	1°	24,200	3°	35,000	50°	13,400	76°	144,000	13°
EXP	-222,000	418,000	-5°	31,700	20°	32,100	34°	39,000	67°	146,000	13°
STA 370 FLAP (IN-LB)											
ANALYSIS	-145,000	47,300	121°	34,600	6°	35,700	102°	29,000	79°	32,800	54°
EXP											
STA 370 CHORD (IN-LB)											
ANALYSIS	-36,700	84,500	3°	8,960	5°	6,500	50°	3,900	78°	4,300	13°
EXP											
SHAFT TORQUE (IN-LB)											
ANALYSIS	7,400	807	0°	3,150	82°	1,200	118°	7,800	30°	2,800	5'
EXP	25,000	14,300	150°	5,800	29°	8,800	40°	19,400	96°	2,400	32°

TABLE VI. MOD-0 CORRELATION STUDY - 0 kW, 20 RPM

HARMONIC / LOAD	0P	1P		2P		3P		4P		5P	
	AMP	AMP	Φ	AMP	Φ	AMP	Φ	AMP	Φ	AMP	Φ
STA 40 FLAP (IN-LB)											
ANALYSIS	-299,000	268,500	137°	58,900	175°	114,100	100°	94,700	47°	147,200	31°
EXP	-223,000	291,000	101°	46,800	136°	26,600	135°	103,600	63°	66,000	44°
STA 40 CHORD (IN-LB)											
ANALYSIS	-123,300	427,000	5°	23,400	174°	6,100	94°	36,500	46°	44,300	1°
EXP	-147,000	437,600	5°	39,700	137°	23,000	32°	26,400	44°	34,200	17°
STA 370 FLAP (IN-LB)											
ANALYSIS	-102,600	65,700	131°	17,900	175°	33,200	102°	30,400	48°	51,700	33°
EXP											
STA 370 CHORD (IN-LB)											
ANALYSIS	-37,000	80,800	10°	8,740	175°	4,900	100°	12,100	47°	9,200	1°
EXP											
SHAFT TORQUE (IN-LB)											
ANALYSIS	730	128	145°	3,000	78°	121	64°	29,800	89°	76	63°
EXP	19,900	22,900	129°	9,800	64°	11,400	95°	16,000	41°	16,500	37°

Good correlation is shown for all the harmonics for the condition of Table III with the exception of the 4P and 5P inplane/chordwise bending moments. Similar results are obtained for the 100 kW - 40 rpm conditions shown in Table IV.

Table V shows a comparison of the harmonics of the same flapwise and inplane/chordwise bending momnets and rotor torque for the 0 kW - 30 rpm condition, and Table VI gives the comparison of loads for the 0 kW - 20 rpm. Good correlation is obtained at all three rotor speeds. The peak flapwise bending moment, at the higher rotor speeds, is underpredicted by approximately 15 percent, see Figure 10.

The "first emergency feather" case was selected for transient correlation. The results of transient REXOR-WT analysis are presented in plotted time history compared with experimental data is shown in Figure 11.

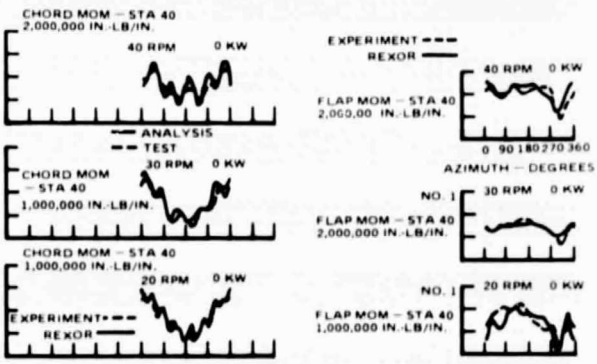

Figure 10. Time History Comparison of REXOR - Wt and Experimental Data

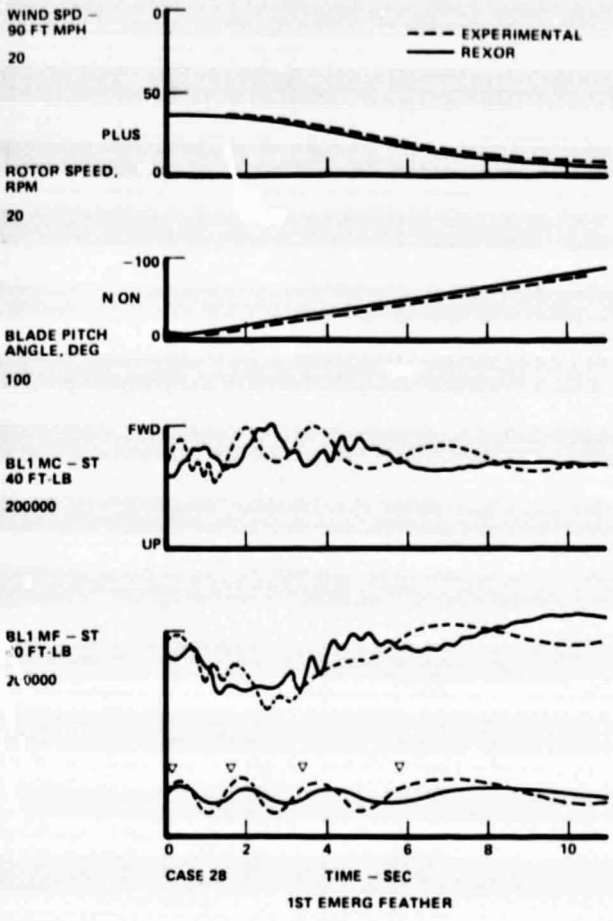

Figure 11. Time History of "First Emergency Feather"

At a selected time, the blade pitch angle was commanded to feather and thereby stop the rotor. The time was selected to attempt to have the initial rotor indexing correspond to the experimental azimuth indexing.

Figure 11 shows the comparison of blade angle and rotor speed. Note that the predicted rotor speed decay is analytically faster than the experimental rate. This difference causes the relative phasings of the analysis and experimental loads to shift with time since load amplitudes are azimuth dependent. This shift in phase is best illustrated by the sine waves of rotor azimuth (predicted and experimental) plotted on the bottom of Figure 11. This means that the correlation should be directed at an envelope of loads, not at the relative load phasing.

Figure 11 also shows a comparison of the experimental and predicted time histories of flap and inplane bending at station 40. Note the fairly good comparison of moment amplitudes.

The drive shaft 4P oscillatory loads problem appears to be associated with the variable spring rate of the low speed shaft flex coupling. A coupler of variable torsional stiffness connects the windmill shaft to the gear train that drives the generator. The stiffness varies with output torque so that the low frequency generator-blade natural frequency varies (see Fig. 12 and Ref. 8) from just above 3P to just above 6P as power output varies from 100 kW to zero at full rpm. This causes torsional resonant oscillations of the generator at 4P at power or torque output levels within the useable range, as indicated in this figure. Two solutions to this problem, in the way of configuration changes, appear to be feasible:

- Increase the coupler stiffness sufficiently to raise the natural frequency of the mode to an acceptable level (being careful to not drive it into the 6P region), or
- Add a torsional damper across the coupler that increases damping in the mode to greater than 10 percent of critical.

Figure 13 shows the variation in natural frequency and mode shape of the 1st and 2nd torsional/rotational modes as the coupling stiffness is increased. The modes are shown with unit blade tip deflections, δ. The equivalent generator armature rotation $\psi_{Gequiv.}$, shown is the actual armature rotation factored by 1/gear ratio. The low frequency modes are characterized by generator torque moments opposing blade deflection moments, while the high frequency modes are characterized by blade and generator armature moments opposing the rotor hub motion moments. Mode 2 is seen to be a rotor 1st inplane collective mode that has a rotational frequency of approximately 10P and is not likely to cause serious resonance problems. (However, it too should be detuned from an even integer value of P).

The low frequency mode (Mode 1) resembles a simple two-spool mode, and as such possesses a generator torque transmissibility that changes little with shaft torsional stiffness. Transmissibility actually reduces somewhat with increasing shaft stiffness due to blade bending. If the coupling stiffness is increased and made more nearly independent of shaft torque, the system can be detuned. A disadvantage to this solution is that the resonant frequency might still cross the 6P line during speed-up to and slow-down from operating rpm, and large oscillations could occur if the rpm dwelled at a critical value for any length of time. These would be amplitude-limited only by generator damping and not by the non-linearity of the spring as they appear to be at present.

The second solution, that of employing a damper while leaving the coupling in its present configuration, would not eliminate the 4P resonance but could attenuate its amplitude to an acceptable level. The damper would also attenuate vibrations at other frequencies.

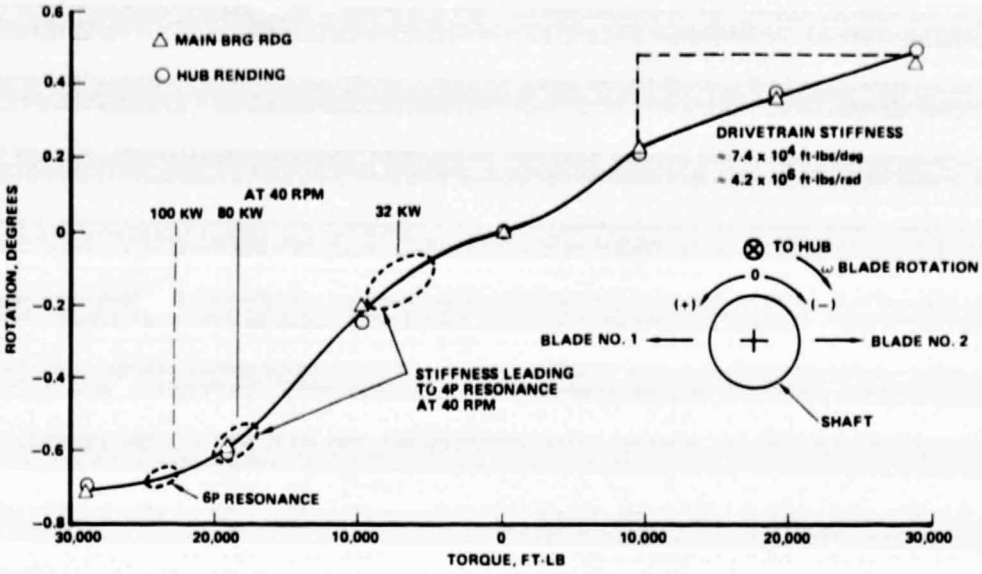

Figure 12. Drivetrain Stiffness

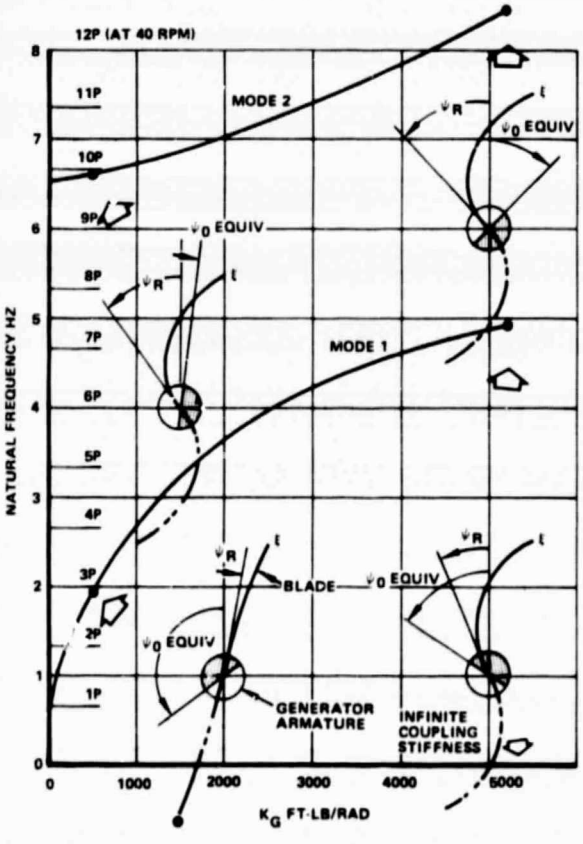

Figure 13. Generator Armature, Shaft and Wind Turbine Blade Natural Vibration Modes and Frequencies vs Shaft Stiffness

Conclusions and Recommendations Based on Test/Analysis

- Accurate prediction of blade loads, particularly at higher frequency, requires an accurate description of tower, nacelle, and drive train dynamics.
- Blade high frequency mode tuning can be significantly affected by the structural dynamics of the tower and nacelle. Chord bending must be monitored if nacelle yaw system characteristics are changed to assure that blade loads don't become excessive.
- Good agreement between calculated and measured loads was obtained in an analysis that included only two blade dynamic modes, first flap and first inplane, and a blade quasi-steady torsion mode.
- Operation of the WTG, in its present configuration, should avoid power and rpm combinations that result in generator-armature resonance.
- To eliminate the armature resonance problem, use of either an increased stiffness coupling or an across-coupler damper appears feasible. Further analyses would aid in making a choice and are required to ensure an adequate design.

OPERATION EXPERIENCE AND EXPERIMENTAL DATA

It was apparent that certain redesign actions were needed to reduce the rotor blade loads. Even though the estimated level of blade fatigue damage was small, further operation in Configuration I would lead to a significantly shorter blade fatigue life than planned. Lockheed determined that less than 10 percent of the fatigue life of the blades was expended during operation in Configuration I.

NASA-LeRC decided to remove the stairs in the center of the tower structure. The stairs were used to provide access from the ground to the nacelle, on top of the tower, that houses the rotating machinery.

Also, two structural rails were removed from one side of the tower. The rails were used to guide a cable car that also provided access to the top of the tower. The increased air flow tends to smooth transitory air loads on the rotor blades as they sweep from freestream into the airflow on the downwind side of the tower. The expected improvement is from almost a 100 percent velocity deficit to only a 25 percent velocity loss, based on both wind tunnel test and laser doppler velocimeter measurements. This configuration, designated II, was then tested at very similar wind conditions to facilitate comparison with the original test configuration I.

Rotor Loads for Configuration II. With the Mod-0 wind turbine in configuration II, the machine was operated at 40 rpm and data was taken as shown in Figure 14. The flapwise and chordwise blade bending moments at station 40 are shown in Figure 14. Blade station 40 is located 40 inches from the center of rotation, measured along the blade radial centerline. Seven cycles of flapwise and inplane bending moments were analyzed. The seven cycles

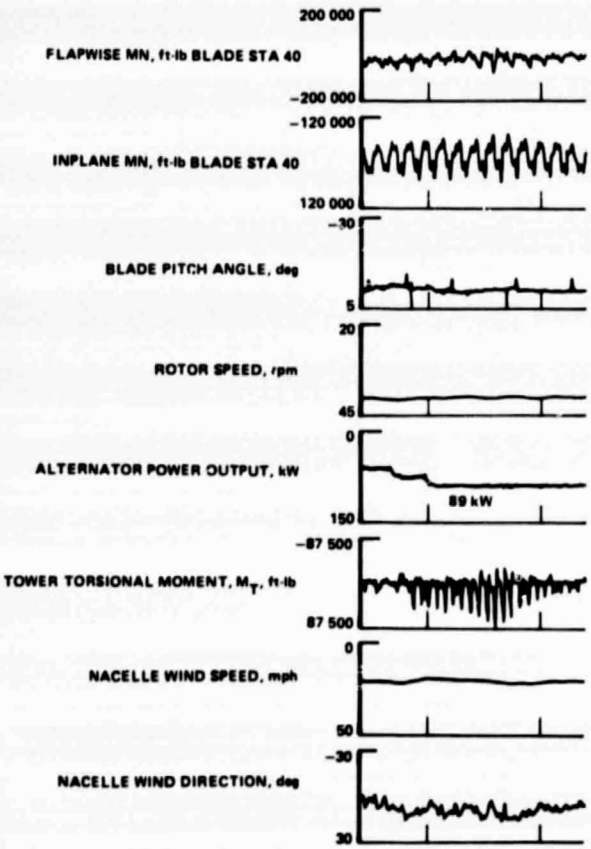

Figure 14. Operation in Configuration II

selected fall between the two vertical parallel lines shown in Figure 14. During that time period, the blade pitch angle maintained an average value of -2°. The blade pitch angle was controlled to maintain constant rotor angular speed (rpm). The alternator power into the resistive load bank was manually set at 89 kW. Because the winds were quite variable, as shown in Figure 14, it was difficult to manually control maximum power, also shown in Figure 14, while maintaining 40 rpm. The wind direction angle with respect to the nacelle angular position, (inflow angle) shown in Figure 14, fluctuated between 3° and 15° during the time period selected. The average inflow angle was estimated at about 10°. The torsion moment measured between the nacelle and the tower, Figure 14, fluctuated to high values. The natural frequency of the nacelle drive mechanism has been analyzed as being close to the frequency of the yaw torque loads produced by the rotor blades. For this reason, the peak values of the yaw torsion loads are seen to amplify and attenuate over the time period considered. NASA-LeRC was concerned that these high peak loads occurring in the yaw drive mechanism would significantly reduce its fatigue life.

Redesign of the yaw drive mechanism appeared necessary. Analyses conducted for NASA-LeRC by Lockheed Aircraft Corp. indicated that if the torsional stiffness of the single yaw drive mechanism was increased, an attenuation of inplane blade cyclic bending moments would occur.

A yaw keeper was originally designed and installed on the Mod-0 wind turbine to restrain the nacelle in the yaw direction as a safety precaution, during assembly or disassembly of the yaw drive mechanism. The yaw keeper, when installed, provides a torsional coupling between the tower and nacelle that is stiffer than the single yaw drive mechanism. Because the yaw keeper was available for use, and because it provided added torsional stiffness, NASA LeRC decided to conduct operational tests on the Mod-0 wind turbine with the yaw keeper installed.

Rotor Loads for Configuration III. With the Mod-0 wind turbine in configuration III, the machine was operated at 40 rpm, producing 100 kW into the resistive load bank. The data is shown in Figure 15.

The flapwise and chordwise blade bending moments at station 40 are shown in Figure 15. Ten cycles of flapwise and inplane bending moments were analyzed. The ten cycles selected are banded by the two vertical parallel lines. During that time period the blade pitch angle, shown in Figure 15, maintained an average value of -3.5°. The wind direction angle with respect to the nacelle angular position, Figure 15, fluctuated between -8° and -16° over the time period selected. The average value is estimated at -12°. The yaw keeper, when installed, only allows one angular position of the nacelle with respect to the tower structure, or ground. The nacelle is positioned at 257° from grid north position. This restricts the operation of the Mod-0 to the time periods when the wind

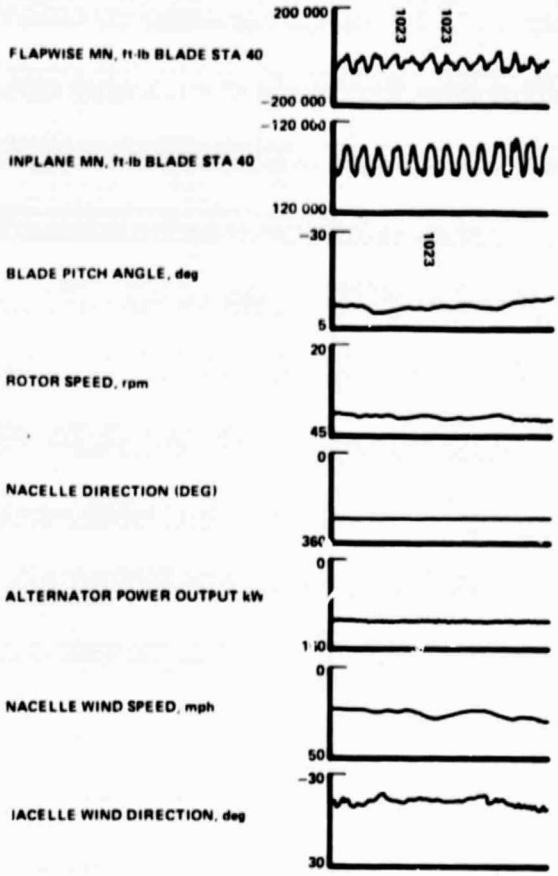

Figure 15. Operation in Configuration III

direction is from the South-West. This position was selected because the most predominate wind direction is from the South-West at the wind turbine site.

The yaw keeper design prevented a close match of the wind inflow angles measured during operation of the wind turbine for configurations I and II. A wind inflow angle of -12° was experienced during operation in configuration III, while a +10° inflow angle was estimated during operation in configurations I and II.

As a result of these test data and a need to reduce rotor blade loads during Mod-0 operation, NASA-LeRC designed and assembled a new yaw drive unit. The unit was installed on the Mod-0 wind turbine in March 1977 for operational tests.

The yaw drive design has two features, as described below.

1. Two yaw drive mechanisms were used, rather than one, and is called the "dual yaw drive unit." Two electric motors and two gear boxes, used to drive the nacelle in yaw, are shown in Figure 3. The dual yaw drive is mounted to a test stand in this figure. The test stand was used to build up the unit and to run operational tests prior to assembly on the wind turbine. This design provides higher stiffness between the nacelle and tower than the single yaw drive design. The single yaw drive allowed about .12° degree in yaw free play. The dual yaw drive was designed to reduce the free play by preloading the drive shafts, in torsion, one against the other.

2. In Figure 4, three hydraulic disc brakes are shown. When the disc brakes are applied, a friction lock is obtained between the tower and nacelle. This system was designed as a replacement for the yaw keeper. The disc brake system allows any desired locked orientation of the nacelle and rotor blades with respect to the wind direction. In addition the disc brake design provides variable yaw moment stiffness in excess of that provided by the double yaw drive.

Comparison of Blade Loads During Operation in Configuration I, II and III

The average blade loads measured during operation in configuration I. II and III are shown in Table I.

On comparing flapwise blade bending moments for configuration I and II the observations are listed below.

1. The average cyclic flapwise bending moment was reduced by 46 percent during operation in configuration II.

2. The mean flapwise bending moment was reduced by 73 percent during operation in configuration II.

The average peak to peak, mean and cyclic inplane bending moments experienced during operation in configuration II were somewhat smaller than the loads measured during operation in configuration I. These results indicate that removal of the tower stairs and rails has a pronounced effect on reducing the flapwise bending moment loads in the rotor blades. However, configuration II had little effect on reducing the inplane bending moment loads in the rotor blades.

On comparing inplane blade bending moments for configuration II and III, the observations are listed below:

1. The average cyclic inplane bending moment was reduced by 22 percent during operation in configuration III.

2. The mean inplane bending moment increased by 75 percent during operation in configuration III.

The average peak to peak, mean and cyclic flapwise bending moments experienced during operation in configuration III are smaller than the loads measured during operation in configuration II.

These results indicate that by increasing the yaw stiffness of the structure between the nacelle and tower, the cyclic inplane blade bending moments can be significantly reduced. However, configuration III had little effect on reducing the cyclic flapwise blade bending moments, when compared to the blade loads encountered during operation in configuration II.

Synchronous Operation - Power/Drive Train Dynamics

Figures 16, 17 and 18 present data representative of operation on a large power grid. Each of the figures show time histories of blade flapwise and chordwise bending moments, rotor torque, alternator power and current, rotor blade pitch angle and rotor speed.

In synchronous operation, the alternator is essentially locked to the power grid at a fixed speed of 1800 rpm. The wind turbine is therefore constrained to operate at a fixed speed dictated by the mechanical advantage between the wind turbine and the alternator. Any tendency on the part of the rotor to vary from this fixed speed is reflected in drive train deflection. The data presented illustrates the effect of drive train flexibility on synchronous operation on the Mod-0 machine.

Initial synchronous operation of the Mod-0 wind turbine was conducted at a 20 rpm rotor speed. This speed was chosen because high rotor blade loads had been encountered at the design rotor speed of 40 rpm. These high blade loads were the result of excessive nacelle yawing motion during 40 rpm operation. Tests at 40 rpm were discontinued until a modification to eliminate this yaw problem could be incorporated. In the meantime, synchronous operation tests at 20 rpm were planned. During these tests, large power oscillations were encountered at this "off-design" rotor speed.

The power oscillations were attributed to a drive train resonance at 40 rpm, or twice the rotor speed of 20 rpm. The resonant response is driven by the excitation of rotor torque caused by tower shadow. A plot of calculated rotor torque versus rotor position for a 40 rpm rotor speed is shown in Figure 19, and is illustrative of the torque characteristics for all rotor speeds. This torque as the driving force of the rotor will result in an impulse each time a blade passes behind the tower. The drive train must either store this torque impulse or transmit it to the generator which will result in a power fluctuation.

In the case of the Mod-0 test at 20 rpm, the torque impulses occurring at 2 times the rotor speed (2P) coincided with the drive train natural frequency, and the impulse loads were amplified to create a power oscillation with a peak-to-peak value approximately equal to the power set point as shown in Figure 16. As indicated in the figure, blade loads were not significantly affected by the power oscillations, but rotor torque was a direct analog of the power trace. The tuned power oscillations have been generally at 2P and exhibit a beating tendency with a 10 to 20-second period.

The oscillations were obviously due to drive train resonances at the 20 rpm rotor speed and it was predicted that operation at 26.3 rpm would separate the forcing frequency from the drive train resonance (i.e., drive train resonance at 40 cpm, forcing function 2x26.3 = 52.6 cpm) and reduce the magnitude of the oscillation. The results of these tests at 26.3 rpm are shown in Figure 17. No improvement resulted from the change in rotor

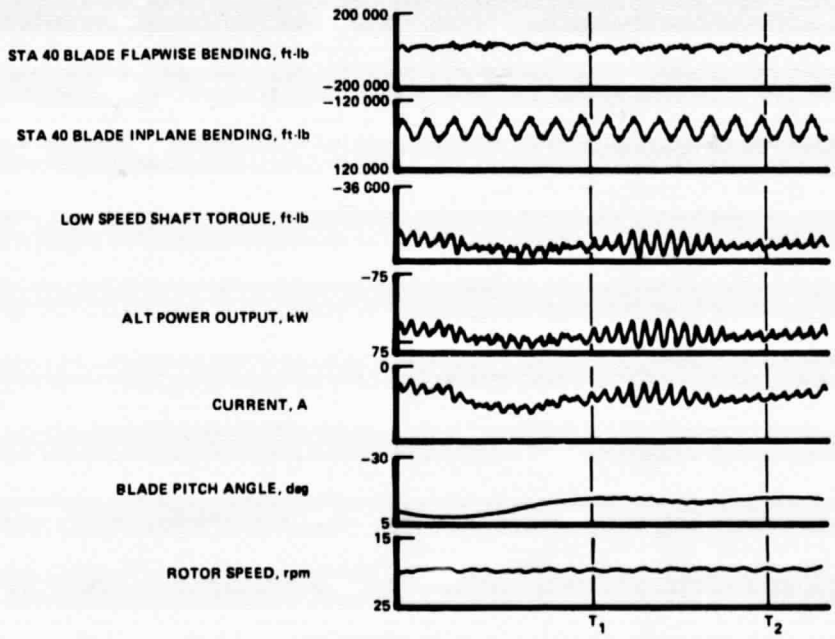

Figure 16. 20 RPM Synchronous Operation

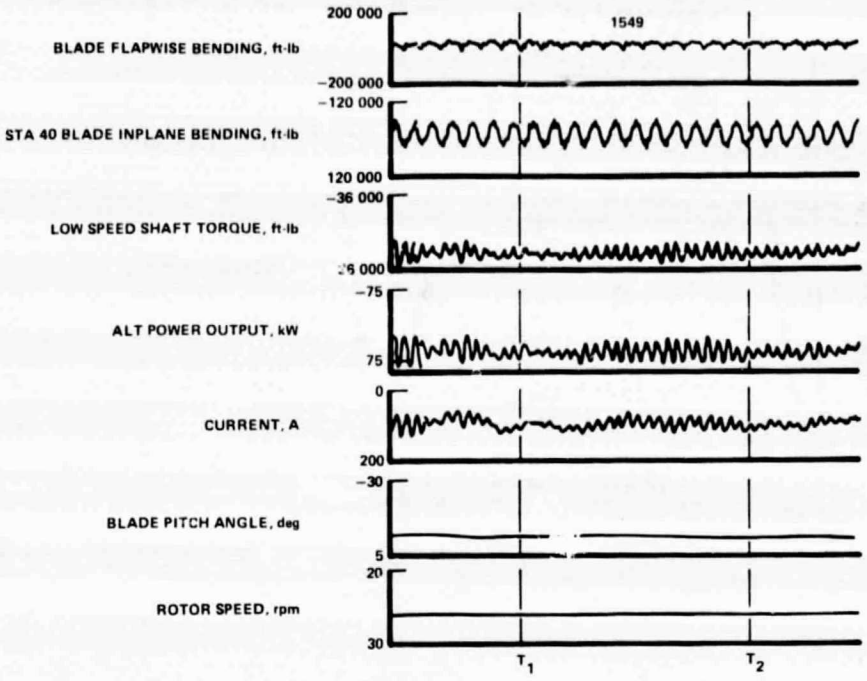

Figure 17. 26.3 RPM Synchronous Operation

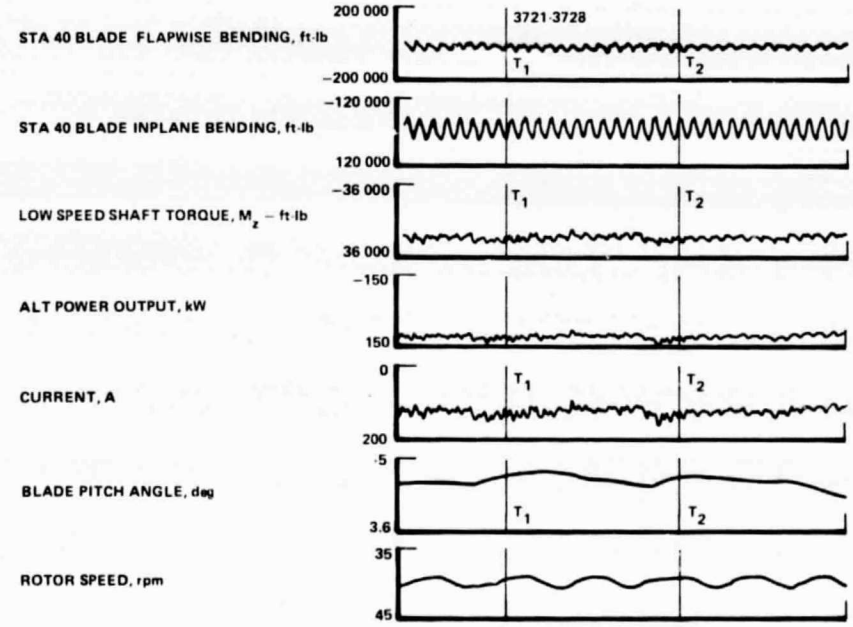

Figure 18. 40 RPM Synchronous Operation

speed as predicted and we concluded that the expected result could be explained by the non-linear spring characteristics of the low speed shaft coupling, resulting in a drive train which would produce a resonance response over a broad frequency range.

After these results were obtained, it was felt that an increase in the rotor speed to 40 rpm, the design speed, would demonstrate a marked reduction in power oscillations. Due to the problems with the yaw restraint, mentioned above, these tests were conducted with the nacelle locked

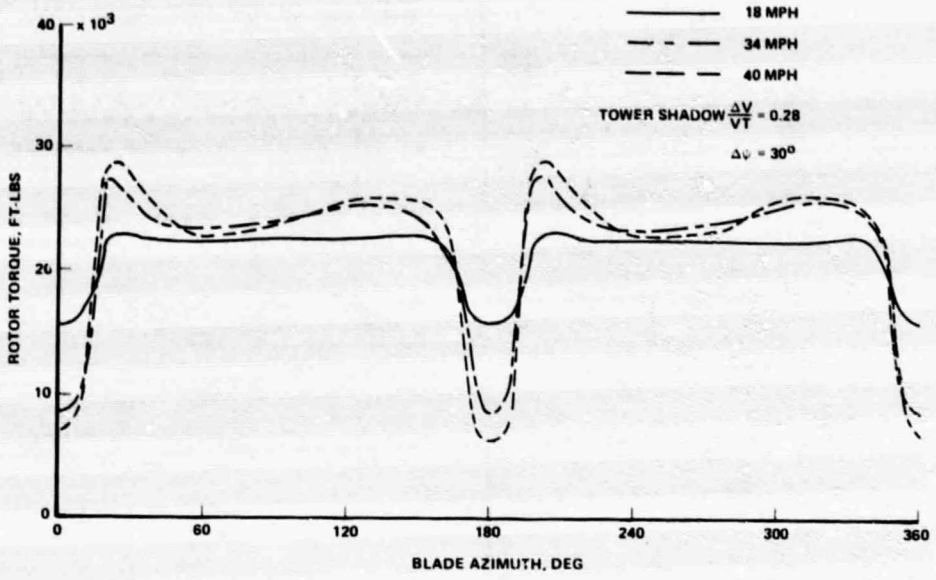

Figure 19. Rotor Torque vs. Blade Azimuth MOSTAB - Wt W/O Stairs 100 kW

to the tower. (Tests at 26.3 rpm with and without the nacelle locked to the tower indicated that this had no effect on 2P power oscillations.) As indicated in Figure 18 the power oscillations have been greatly reduced at the 40 rpm rotor speed.

Tests at 40 rpm rotor speed produced a more favorable separation between drive train frequency and forcing frequency making the drive train appear more compliant or softer and permitting more of the torque variations to be stored in the drive train. An indication of the effect of the softer drive train is shown by comparing the rotor speed traces in Figure 16, 17 and 18. Rotor speed is measured on the low speed shaft at the gear box. At 20 rpm the rotor speed is rather steady and variations do not exceed 1 rpm peak to peak. At 26.3 rpm rotor speed is very steady and at 40 rpm the rotor speed exhibits variations approaching 2 rpm peak-to-peak. These tests indicate that a very soft highly compliant drive train will minimize power oscillations and will result in a smoother operating machine. This conclusion has been borne out by drive train analysis and hardware is being fabricated. The modified drive train will have its resonant frequency reduced by a factor of two and will have increased damping. This modification should result in an improved power trace throughout the range of rotor speeds from 20 rpm to 40 rpm. Other means of incorporating drive train flexibility are being investigated. Promising techniques will be evaluated in the Mod-0 program.

Additional system test results including blade loadings in the ERDA-NASA 100 kW Mod-0 as well as analysis of the 200 kW Mod-0A Wind Turbine, now being assembled for installation as part of the municipal power plant of Clayton, New Mexico, is reported in Reference 9.

REFERENCES

1. Puthoff, Richard L.: Fabrication and Assembly of the ERDA/NASA 100 Kilowatt Experimental Wind Turbine. NASA TM X-3390, 1976.

2. Glasgow, John C.; and Linscott, Bradford S.: Early Operation Experience on the ERDA/NASA 100 kW Wind Turbine - Rotor Blade Loads. NASA TM X-71601, 1976.

3. Cherrit, A. W.; and Gaidelis, J. A.: A 100 kW Metal Wind Turbine Blade Basic Data, Loads and Stress Analysis. (LR-27153, Lockheed-California Co.; NASA Contract NAS3-19235.) NASA CR-134956, 1975.

4. Donham, R. E.; Schmidt, J; and Linscott, B. S.: 100-kW Hingeless Metal Wind Turbine Blade Design, Analysis and Fabrication. Presented at the 31 st. Annual National Forum, American Helicopter Society, (Washington, D.C.), May May 13-15, 1975.

5. Friedman, P. P.: Aeroelastic Modeling of Large Wind Turbines. Presented at the 31 st. Annual National Forum, American Helicopter Society, (Washington, D.C.), May 13-15, 1975.

6. Ormiston, Robert A.: Rotor Dynamic Considerations for Large Wind Power Generator Systems. Wind Energy Conversion Systems, J. M. Savino, ed., NASA TM X-69786, 1973, pp. 80-88.

7. Anderson, W. D.: A 100 kW Metal Wind Turbine Blade Dynamics Analysis, Weight/Balance, and Structural Test Results. (LR-27230 Lockheed-California Co.; NASA Contract NAS3-19235.) NASA CR-134957, 1975.

8. Sulivan, T. L.; Miller, D. R.; and Spera, D. A.: Drive Train Normal Modes Analysis for the ERDA/NASA 100-Kilowatt Wind Turbine Generator. ERDA/NASA/1028-77/1, NASA TM-73718, 1977.

9. Spera, D. A.; Janetzke, D. C.; and Richards, T. R.: Dynamic Blade Loading in the ERDA/NASA 100 kW and 200 kW Wind Turbines. NASA TM-73711, 1977.

10. Crockett, H. B.: Wind Turbine Towers, 1/50-Scale Model Tests at CALCIT. (Motion Picture, 17 minutes, color/sound). LAC/047485, Lookheed-California Co., Mar. 25, 1976.

11. Bettes, W. H.: Report on Wind Tunnel Tests on 0.020-Sa Scale Models of Several Types of Wind Turbine Towers. Rep. 972, Graduate Aeronautical Labs., California Institute Technology, Pasadena, Apr. 2, 1976.

12. Savino, Joseph M.; and Wagner, Lee H.: Wind Tunnel Measurements of the Tower Shadow on Models of the ERDA/NASA, 100 kW Wind Turbine Tower. NASA TM X-73548, 1976.

APPENDIX A

Description of the 100-kW WTG System

The 100-kW experimental WTG consists of a two-bladed, horizontal-axis, rotor system driving a synchronous electric generator through a step-up gear box. This equipment is mounted on top of a 100-foot tower as shown in Figure A-1, with the rotor located downwind from the tower. The rotor-turbine operates at 40 rpm generating 100 kW of electrical power with an 18-mph wind velocity measured at the rotor-turbine axis height.

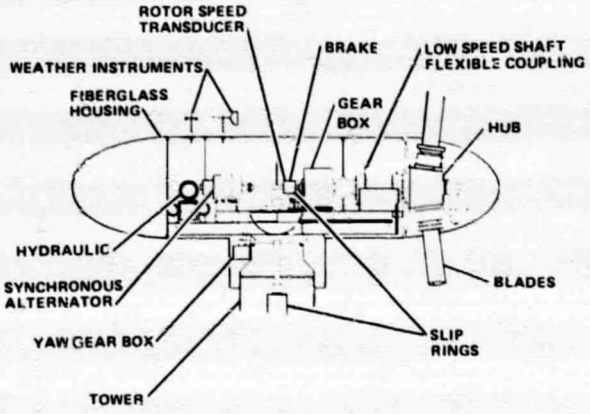

Figure A-1. 100 kW Experimental Wind Turbine Generator

The hub and blades are mounted on a shaft which drives a speed-up gear box. In the gear box, the shaft rpm is increased from 40 to 1800 rpm. A high-speed shaft connects the gear box to the 100-kW alternator.

The 125-foot-diameter hingeless rotor has two aluminum blades designed to provide 133 kW of shaft power at 18 mph wind speed when rotating at 40 rpm. They have a 33.8 degree nonlinear twist with a NACA 23000 series airfoil.

The pitch change mechanism consists of an hydraulic pump, a pressure control valve, actuator and gears for rotational movement of the blades. This mechanism is similar to that used on some aircraft propellers. At wind velocities above 18 mph, the rotor blades increase pitch, thus spilling the wind and ensuring that the electrical power developed does not exceed 100 kW. Below 8 and above 60 mph the turbine blades will be placed in a feathered position and the machine shut down.

The tower, 100 feet tall, is an open steel truss structure secured to a steel-reinforced concrete foundation. The WTG equipment at the top of the tower is designed to rotate (yaw). Yaw control allows alignment of the rotor with the wind direction. Yaw rate is 1/6 rpm and is operational when the machine is or is not generating power. This allows alignment with wind direction changes that occur with the passage of a weather front, but not with random variation of wind direction due to gusts.

The tower was designed by the NASA-LeRC Facilities Engineering Division. In recognition of the importance of this experimental facility to the testing of future systems, the possibility of dynamic interaction between the rotor and tower has been minimized by designing the structure with high stiffness and high natural frequency. A NASTRAN model of this system has been formulated and the results of the dynamic analysis show that the first bending natural frequency of the tower/rotor is 2.5 Hz (3.75P at 40 rpm).

The elastic characteristics of the support shaft, bedplate, and tower have been coupled to the rotor system, and blade spectrum frequencies as well as flutter stability solutions obtained. Since the characteristics of the tower support are asymmetric and rotor is two-bladed, the system cannot be treated rigorously by stationary nonrotating system coordinates with constant coefficients, i.e., time variant equations must be solved.

The Lockheed-California Company began work in September 1974 under Contract NAS3-19235 on the 100-kW WTG blades. This contract provided for design, analysis, fabrication, instrumentation, and shake-testing of three blades (set of 2 with one spare). Blade geometry is shown in Figure A-2.

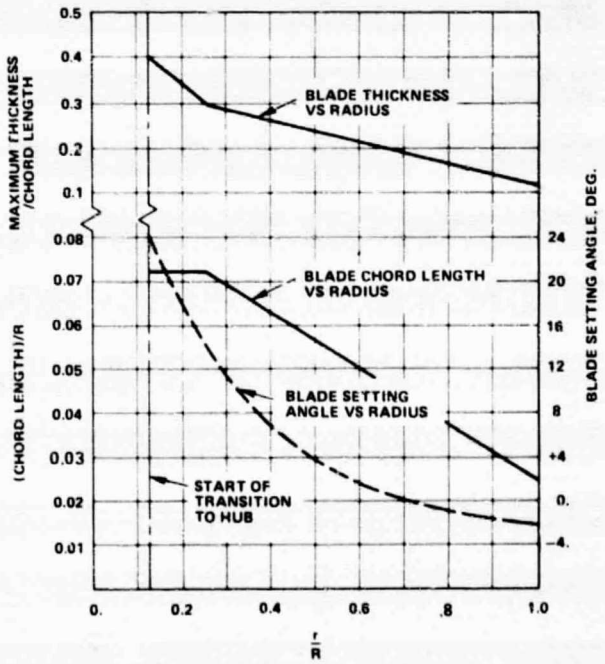

Figure A-2. Blade Geometry

The use of spars, ribs, stringers, heavy nose skins, light trailing-edge skins (thickness determined by avoidance of hail damage), the root-end fitting and the two heavy machined ribs is derived from conventional aircraft design/fabrication technology. A D-spare structural concept was used which provides strength, rigidity, balance and low weight; these

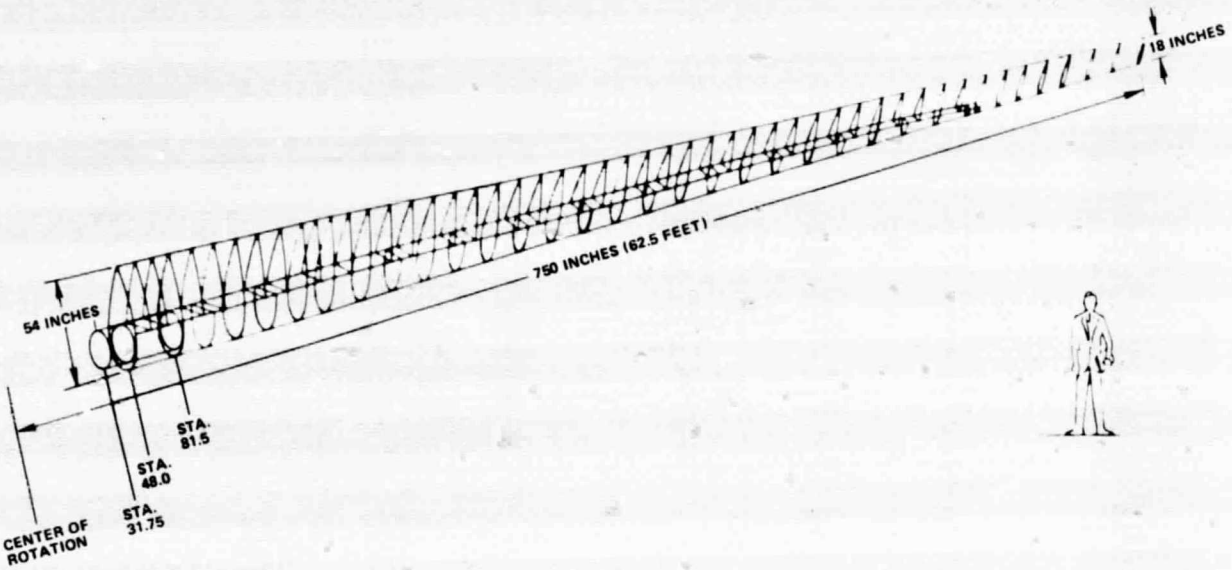

Figure A-3. 100-kW Wind-Turbine Blade

qualities are also consistent with rotary wing designs. Figure A-3 shows general structural dimensions for each blade.

In the design of a rotor system, detailed consideration must be given to dynamic characteristics. Items that generally require attention are frequency placement, flutter including wake effects, torsion-flap-inplane stability, stall flutter, gust response, and effect of tower support and control system characteristics on coupled rotor-tower dynamic stability, response, clearance, and transient loads associated with system response during starting and stopping.

The cantilevered blade frequency spectrum from 0 to 80 rpm is presented in Figure A-4. These results are for the fully coupled flapping - inplane bending and torsion description.

The distributed inertia characteristics of the blade, described as a lumped parameter system, are given in Table A-I. Calculated structural stiffness curves for the distributed flap bending, inplane bending, and torsion characteristics are presented on Figure A-5.

Non-rotating structural tests were conducted on the first metal wind turbine blade mounted on a test fixture. This support fixture simulated the hub/spindle stiffness of the 100 kW experimental wind turbine generator. The test/analysis frequency summary comparison presented in Table A-II shows that excellent correlation was obtained. The frequencies of the flapping modes and the inplane modes are both slightly higher than calculated which is largely attributed to higher blade bending stiffness levels being obtained. The first torsion mode was slightly lower than predicted, but for a 2000 cpm mode this is good correlation.

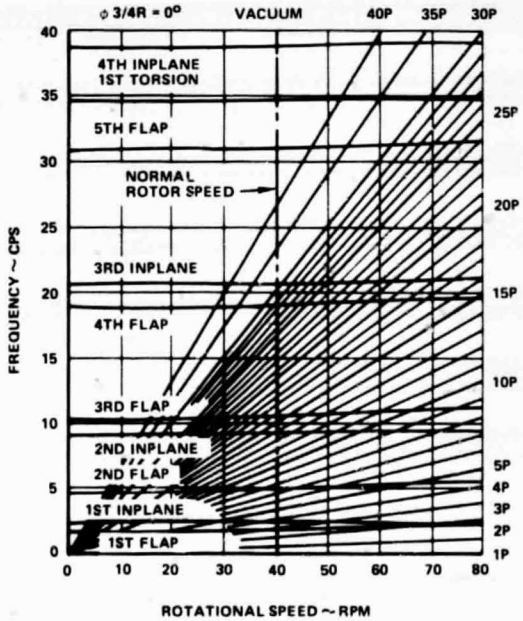

Figure A-4. Wind-Turbine Cantilever Blade Coupled Frequency Spectrum

Mod-0 Wind Turbine Tower Porosity

Mod-0 wind tunnel tower models have been constructed at approximately 1/50 scale and were tested independently by NASA Lewis Research Center and by Lockheed, using rake survey techniques to determine the downstream pressure losses and thereby determine the velocity field characteristics. The velocity distribution of the full-scale system about the tower structure was also measured by a laser Doppler velocimeter system recently developed by Lockheed.

TABLE A-I. METAL WIND-TURBINE BLADE LUMPED PARAMETER WEIGHT DISTRIBUTION

WEIGHT (LBS)	X ARM (IN.)	Y ARM (IN.)	Z ARM (IN.)	I_{XX} (LB IN^2)	I_{YY} (LB IN^2)	I_{ZZ} (LB IN^2)	P_{XZ} (LB IN^2)
138.77	0.00	37.31	0.00	7676	9244	7676	0
188.99	3.11	54.96	0.69	15453	25732	19117	3612
257.64	3.23	79.01	0.74	33631	19668	46594	7757
130.17	1.54	124.89	0.40	29574	26988	39414	3905
135.68	1.58	171.27	0.23	28538	26697	41962	3387
117.69	2.40	213.81	0.36	22323	21834	36461	2381
114.95	1.77	257.66	0.11	21717	17184	32556	1381
55.04	1.62	290.65	0.51	3513	7180	8106	413
68.96	-0.18	312.58	-0.46	4144	9664	11084	700
131.45	-0.36	345.96	-0.12	23018	15446	34842	871
108.01	-0.10	389.04	-0.16	18656	10265	26461	328
109.09	-0.28	433.14	-0.11	18561	8864	25503	178
98.18	-0.27	477.18	-0.08	16432	6823	22070	78
84.39	-0.22	521.19	-0.08	14358	4273	17494	-21
79.11	-0.16	564.96	-0.01	13032	3132	15624	-35
56.05	-0.21	608.22	0.01	9172	2281	11195	-71
20.08	-0.26	642.34	0.00	841	673	1453	-23
15.43	-0.13	663.66	-0.07	643	706	1307	-20
28.58	-0.04	698.11	-0.04	5512	1007	6470	-36
17.28	-0.29	736.45	-0.04	1057	398	1444	-19
1955.54	1.13	269.97	0.63	215264289	225307	215387656	26587

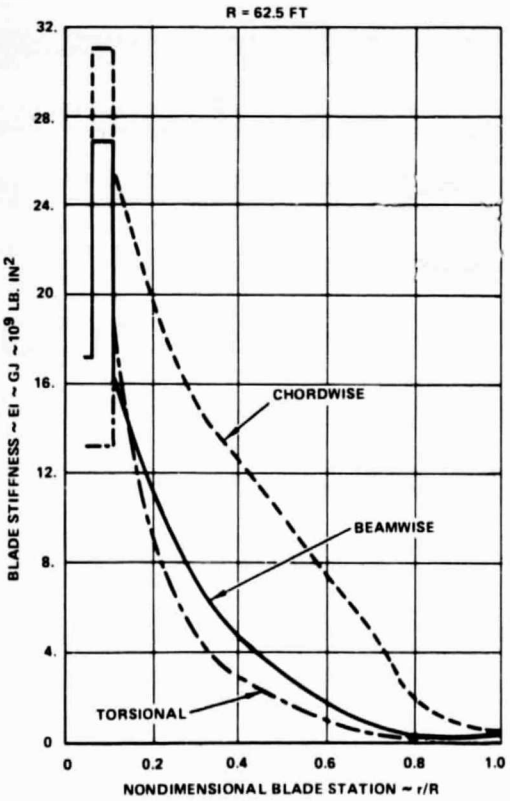

Figure A-5. Wind-Turbine Blade Stiffness Distribution

The NASA Lewis Research Center icing tunnel was utilized in the one case and the Lockheed sponsored tests were conducted at the Wind Tunnel of the Guggenheim Aeronautical Laboratory at the California Institute of Technology in Pasadena, California, under Lockheed independent development funding, Figure A-6, references 10, 11, and 12.

TABLE A-II. METAL WINDMILL BLADE FREQUENCY SPECTRUM DETERMINED BY NONROTATING TESTS

TEST/ANALYSIS FREQUENCY SUMMARY			
MODE SHAPE	FULL TIP WEIGHT* 7.4 LB/BLADE (TEST)	NO TIP WEIGHT* (TEST)	NO TIP WEIGHT (ANALYSIS)
1ST FLAPPING	97.8 cpm	103.8 cpm	98.7 cpm
2ND FLAPPING	280.8 cpm	299.4 cpm	286 cpm
3RD FLAPPING	600.0 cpm	622.8 cpm	610 cpm
1ST INPLANE	141.0 cpm	159.6 cpm	143 cpm
2ND INPLANE	567.6 cpm	588.0 cpm	558 cpm
1ST TORSION	(NOT TESTED)	1968 cpm	2040 cpm
*METAL BLADE WAS PRIMED BUT NOT THROUGH FINAL PAINT; SURFACE AREA WEIGHT WOULD INCREASE BY 25 LB/BLADE.			

Both tests showed almost 100 percent velocity retardation when the tower stairs and rails were present and approximately 25 percent when the stairs and rails were removed.

The Mod-0 tower was also examined at Lockheed by a computer graphics technique to give a visual comparison of porosity as wind direction is changed. Figure A-7 shows the visual impression of porosity versus the actual measured drag from the Galcit tests.

The tower for the 100 kW Mod-0 wind turbine generator is constructed of steel where members are both circular and angular in cross section. The circular sections were used for the near vertical members at the corners. The drag coefficient of a circular cylinder is 1.2 before transition, about two-thirds of the typical, angular structural element. A tower constructed entirely of tubing could be expected to have a smaller wake.

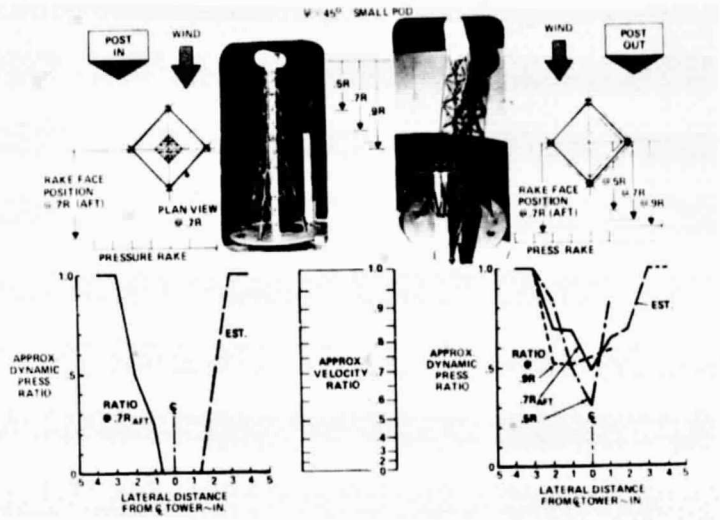

Figure A-6. Conventional Truss Tower

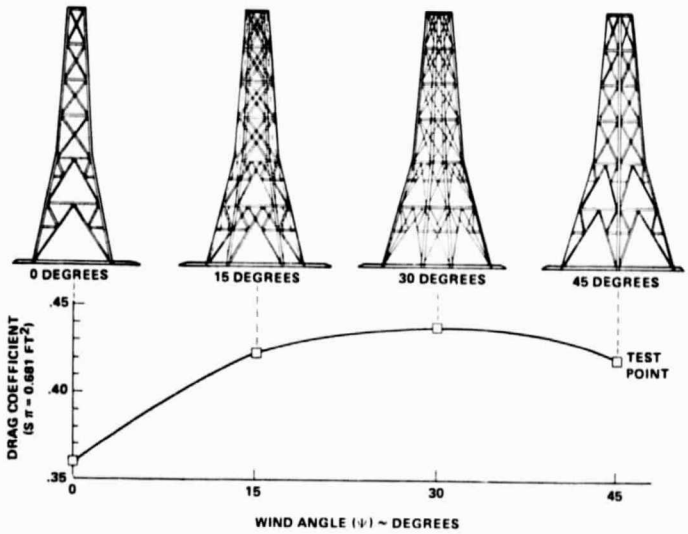

Figure A-7. Comparison of Measured Drag Coefficient With Flow Angle; Mod-0 Tower